



Synthesis of silver-zeolite films on micropatterned porous alumina and its application as an antimicrobial substrate

Supriya Sabbani^a, Daniel Gallego-Perez^b, Amber Nagy^c, W. James Waldman^c, Derek Hansford^b, Prabir K. Dutta^{a,*}

^a Department of Chemistry, The Ohio State University, Columbus, OH 43210, USA

^b Biomedical Engineering Department, The Ohio State University, 1080 Carmack Road, 270 Bevis Hall, Columbus (OH) 43210, USA

^c Department of Pathology, The Ohio State University College of Medicine, 4160 Graves Hall, 333 West 10th Avenue, Columbus, Ohio 43210, USA

ARTICLE INFO

Article history:

Received 29 March 2010
Received in revised form 25 June 2010
Accepted 29 June 2010
Available online 3 July 2010

Keywords:

Patterned membranes
Soft lithography
Micropatterning
Alumina membrane
Antibacterial

ABSTRACT

In this study, we focus on synthesis of patterned-zeolite films and the potential application of a silver-derived form of this film as a biocidal agent. The synthetic strategy has been to develop a patterned porous alumina substrate using soft lithographic methods. These patterns have dimensions in the range of 5–100 μ . Previously patterned PDMS and PMMA molds were used to define surface microfeatures on the alumina supports. Zeolite films (2–3 μ) were then grown on the alumina using a seeding process followed by secondary growth. Electron microscopy showed that the zeolite film followed the pattern of the alumina substrate. Silver nanoparticles were grown on the surface of the zeolite film by reduction of the Ag⁺ – exchanged zeolite with aqueous hydrazine. The antimicrobial properties of the patterned-zeolite films were successfully demonstrated using *Escherichia coli* bacteria as the model system, complete bacteria eradication was noted within 120 min. Such patterned-zeolite films can be incorporated into a variety of systems, including fabrics, biomaterials, filters and thus can serve a wide range of uses.

© 2010 Elsevier Inc. All rights reserved.

1. Introduction

Zeolites are three-dimensional, microporous, crystalline solids with well-defined structure [1,2]. Ion exchange, thermal stability, catalytic properties and modifications of the surface and pores of zeolites makes them attractive candidates for various applications. Zeolites with film/membrane configurations are used in sensor devices [3] and for the separation of gases and liquids [4–6]. Zeolite membranes on ceramic supports have also been successfully employed as catalyst units in reactors [7]. In these applications, an increase in the surface area of the membrane will allow for overall smaller volumes, thus, enabling the design of more efficient and compact operational units. Towards that goal, the development of micropatterned zeolites films provides a novel approach.

Patterning is typically done on materials like silicon using photolithography and etching [8]. Over the last decade, there have been significant developments in non-photolithographic techniques using elastomeric polymers, such as polydimethylsiloxane (PDMS). This field is referred to as soft lithography and includes microcontact printing (mCP), replica molding (REM), microtransfer molding (mTM), micromolding in capillaries (MIMIC), and solvent-assisted micromolding (SAMIM) [9]. Micropatterning of ceramics is

not possible with conventional methods of ceramic forming such as dry pressing, whereas with soft lithography, it is possible to generate micrometer-size features [10–12]. Ceramics on support, as well as free standing structures have been fabricated.

There are several reports on the design and fabrication of micropatterned alumina using soft lithography [13–17]. Free-standing alumina components have been fabricated by filling patterned PDMS molds with alumina slurry, followed by demolding and sintering [13]. The use of mold release agents has been reported for the removal of isopressed alumina bodies from PDMS molds [14]. Micropatterned alumina structures on silicon and sapphire have been reported using patterned photoresist as a mold, which is subsequently removed by dissolution [16]. Embossing and mTM have similarly been reported for making micropatterned alumina structures [17].

There have also been a few reports on the micropatterning with zeolites [18–22]. A strategy involving the creation of patterns on a silicon substrate by photolithography, followed by zeolite growth in the etched microcavities led to micropatterns. The zeolite was selectively grown in the microcavity by surface modification of the silicon with mercapto-3-propyltrimethoxysilane which helped anchor the zeolite seeds. By etching away the silicon, freestanding membranes were formed [18,19,21]. Ultraviolet radiation/ozone illumination through a physical mask of a zeolite film, followed by chemical treatment led to creation of a pattern of isolated zeolite islands on the substrate surface [20]. Other studies have in-

* Corresponding author. Tel.: +1 614 2924532; fax: +1 614 6885402.
E-mail address: dutta.1@osu.edu (P.K. Dutta).

cluded the self-assembly of zeolite nanocrystals around PDMS molds to create micropatterns by a micromolding method [22].

In this paper, we present a soft lithographic technique for making patterned zeolite Y films on a porous alumina support. To the best of our knowledge, this is the first report of a patterned-zeolite film on a porous alumina support, with the zeolite film conformal to the patterned substrate. The synthetic strategy involved formation of a patterned alumina support, followed by a seeded, secondary growth of the zeolite Y film. Ion-exchange of silver ions into the zeolite film was carried out, followed by chemical reduction to form metallic Ag particles. The antimicrobial properties of this patterned Ag-zeolite film towards *E. coli* was examined, and this study suggests that patterned-zeolite film provides a new platform for biocidal applications.

2. Experimental section

2.1. Materials

Silver nitrate (Aldrich), polyethyleneglycol PEG-600 (Fluka), poly(methyl methacrylate) (PMMA) (Aldrich), DARVAN (R. T. Vanderbilt company, Inc), hydrazine (Aldrich), aluminum hydroxide (Alfa Aesar, 80.5%), sodium hydroxide (Mallinckrodt, 98.8%), 25 wt.% tetramethyl ammonium hydroxide aqueous solution (Sachem), Ludox SM-30 (nano, Aldrich), AKP30 high-purity alumina powder (Sumitomo Chemical Co. Ltd., Tokyo, Japan), with an average particle size of 300 nm, Silastic T-2 polydimethylsiloxane (Dow Corning), and 1-octanol (puriss, Fluka, Buchs, Switzerland) were purchased and used without further purification. LB broth powder was purchased from Agros Chemical. Agar was obtained from Fisher Scientific and 24 well plates from Falcon.

2.2. Methods

X-ray powder diffraction (XRD) patterns were recorded with a Rigaku Geigerflex diffractometer using Ni-filtered Cu K α radiation (40 kV and 25 mA). The morphology of alumina supports and zeolite membranes were obtained using a Philips XL-30 FEG scanning electron microscope.

2.3. Alumina suspension

The 80 wt.% alumina slurry was prepared by adding AKP-30 (300 nm) alumina powder to ultrapure water (18 M Ω cm) containing 0.5 mL of dispersant ammonium polyacrylate and 1 mL of polyethylene glycol (binder). The suspensions were ball milled with alumina balls for 24 h followed by addition of two drops of 1-octanol.

2.4. Patterned α -Al₂O₃ supports

Surface microfeatures were defined on the alumina supports using previously patterned PDMS and PMMA molds. Photolithographically-patterned silicon masters with the microfeature geometries to be explored were used to obtain the PDMS molds. Briefly, Silastic T-2 PDMS was mixed with its curing agent at a 10:1 ratio, poured over the patterned masters, vacuum degassed and cured at room temperature for 48 h before removal. Patterned PDMS stamps were then peeled from the master and used to either directly pattern the alumina (Fig. 1), or to create a PMMA mold for subsequent alumina patterning (Fig. 3). For creating the PMMA mold, a 20 wt.% PMMA solution in anisole was drop cast on the PDMS mold and dried for 5–6 h at room temperature followed by peeling off from the PDMS stamp. Patterned alumina substrates were prepared by drop casting the alumina slurry onto the PDMS

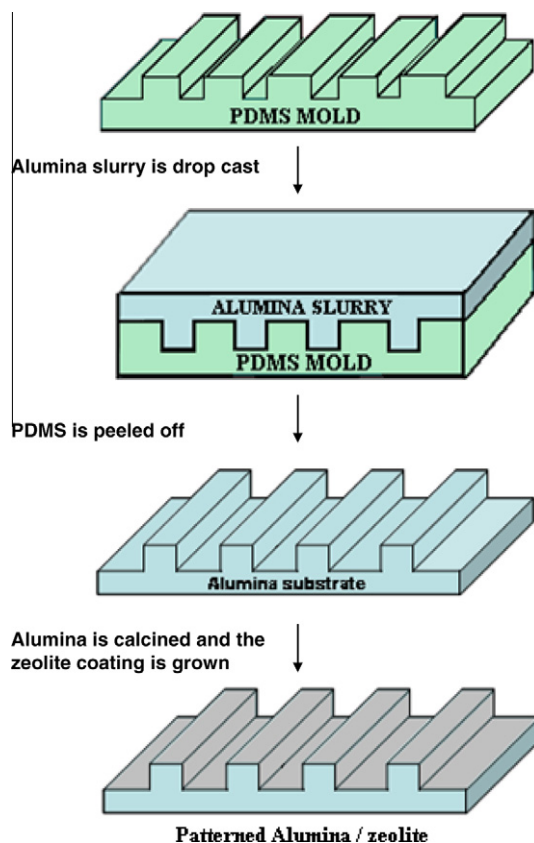


Fig. 1. Schematic diagram of the fabrication of micropatterned zeolite/alumina using a PDMS mold. Alumina slurry is poured onto a PDMS mold, which is peeled off, the alumina fired and then zeolite grown on the alumina using a seeded hydrothermal synthesis method.

or PMMA molds, and drying at room temperature. The PDMS molds were then manually detached from the alumina followed by sintering at 950 °C. Conversely, with the PMMA mold, the alumina/PMMA monolith was heated gradually to 950 °C at ramp rate of 0.2 °C/min. During this sintering process, the PMMA was removed via pyrolysis.

2.5. Zeolite Y synthesis

Nanocrystalline zeolite Y was used as a seed crystal and was synthesized from clear solutions of tetramethylammonium (TMA)-aluminate. The synthesis solution had the following molar composition: 0.037 Na₂O, 1.0 Al₂O₃, 3.13 (TMA)₂O, 4.29 SiO₂, 497 H₂O. The synthesis mixture was placed in a Teflon bottle and heated at 98 °C in an oven until crystals were observed.

2.6. Synthesis of zeolite films on microfabricated alumina supports

An aqueous suspension of the nanocrystalline zeolite Y with a concentration of 3 g/L, pH~8.1, was used to form a seed layer on the patterned surface of α -Al₂O₃ support disks. To accomplish selective one-side coating, the seed suspension was poured in a Petri dish, placed on a height-adjustable lab jack and slowly moved towards the patterned surface of the support disk, until the support touched the suspension. After 5 min of contact, the support was removed and dried for 24 h. This process was repeated three times. These seed layers were grown by hydrothermal reaction in a synthesis solution of molar composition 0.037 Na₂O, 1.0 Al₂O₃, 3.13 (TMA)₂O, 4.29 SiO₂, 497 H₂O at 90 °C. Because of the difference in thermal expansion between the zeolite film and the alumina

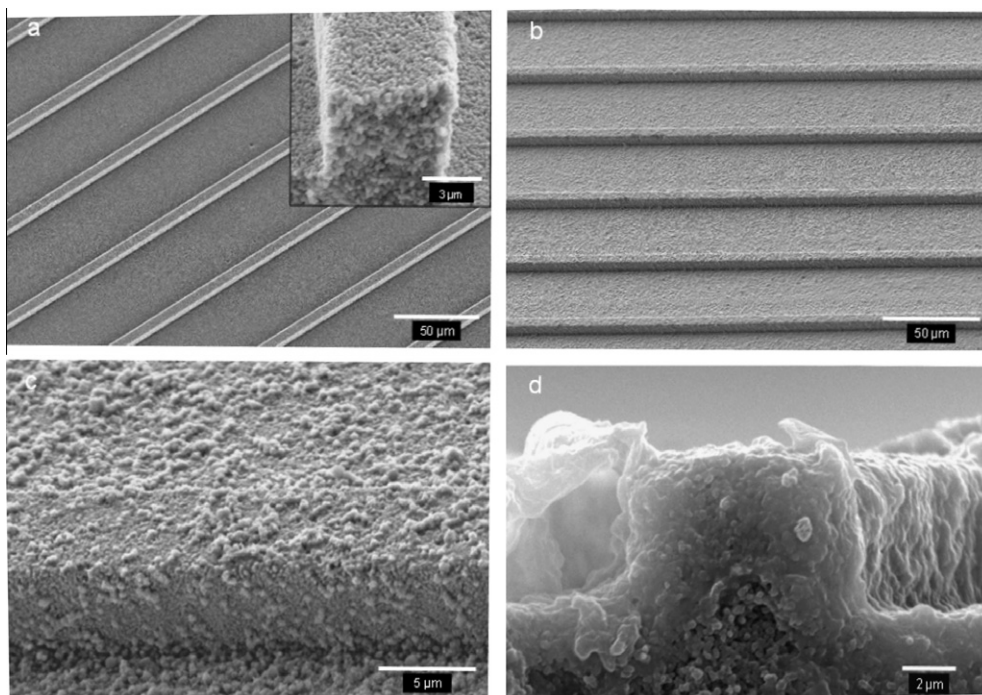


Fig. 2. SEM micrographs of (a) the porous alumina recovered after sintering (inset shows the cross-section of a patterned substrate in the green form) (b) zeolite film grown on the alumina (c) higher magnification image of the zeolite film and (d) cross section view of the zeolite/alumina film showing a zeolite film of 2–3 μm thickness.

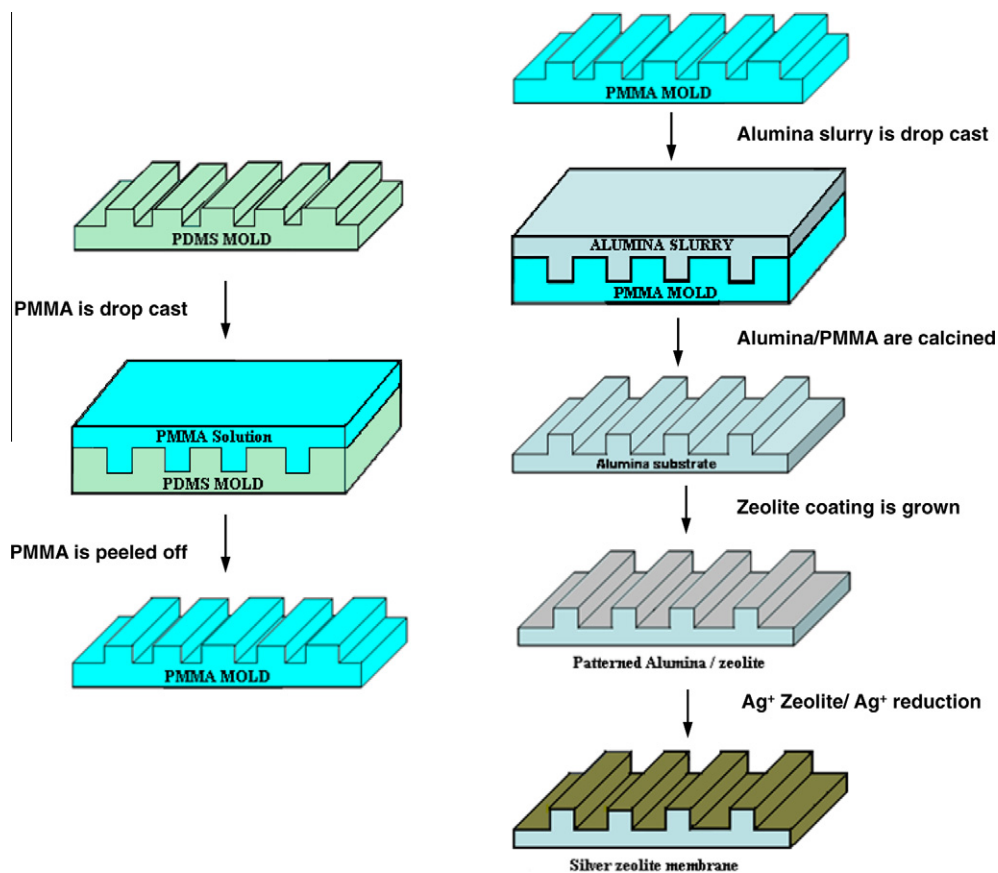


Fig. 3. Schematic description of the zeolite growth using a sacrificial PMMA mold. The PMMA mold is made from the PDMS mold, alumina slurry is cast on the PMMA, the entire composite sintered to densify the alumina and remove the PMMA, followed by zeolite growth on the alumina using a seeded hydrothermal method. The final step involves the formation of Ag nanoparticles on the zeolite surface by ion-exchange with Ag⁺ and hydrazine reduction.

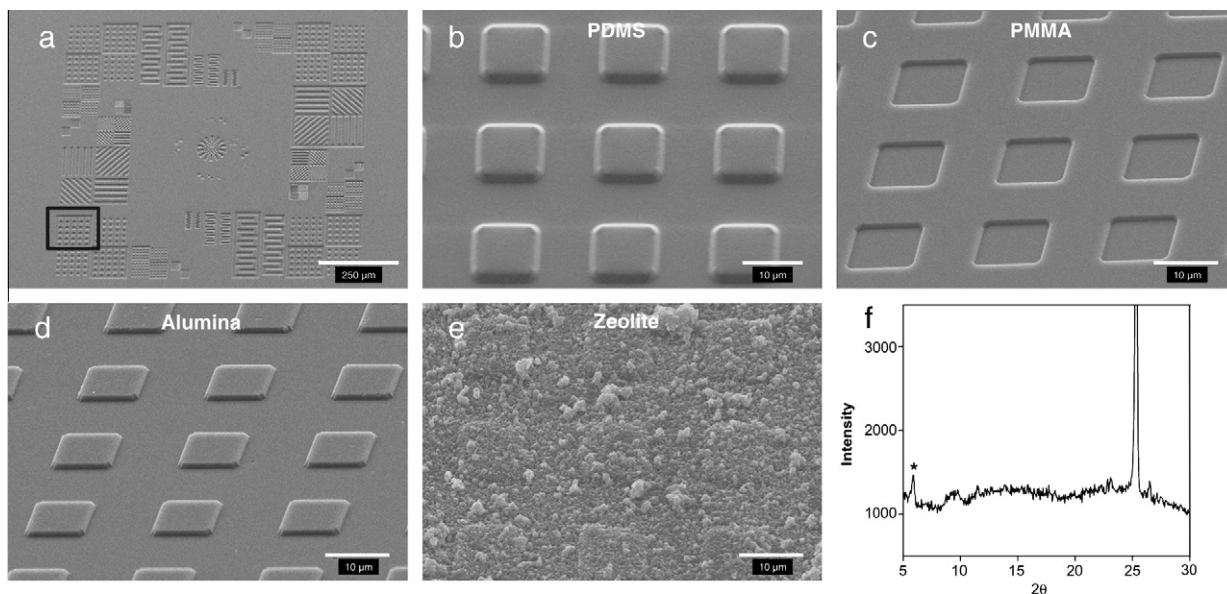


Fig. 4. SEM micrographs of the various stages of growth using the method described in Fig. 3. (a) The PDMS mold made from the silicon mold; the following micrographs focus on the black square shown in the figure (b) the PDMS mold (c) the PMMA replica (d) after alumina deposition, sintering and removal of the PMMA (e) the zeolite film grown on the alumina. (f) X-ray diffraction pattern of the zeolite film (* indicates the (111) reflection from the zeolite, the other strong peak is from the alumina, weaker peaks at 2θ 10, 12, 23 and 27° all arise from the zeolite).

support, the material needed to be calcined carefully in a temperature controlled tube furnace as follows: (1) room temperature to 350°C at $0.2^\circ\text{C}/\text{min}$, (2) maintained at 350°C for 6 h, (3) increased temperature to 450°C at $0.2^\circ\text{C}/\text{min}$, (4) maintained at 450°C for 6 h, and (5) cooled down to room temperature at $0.5^\circ\text{C}/\text{min}$.

2.7. Silver particles formation on patterned-zeolite films

Calcined, patterned-zeolite films were sodium exchanged with 1 M NaCl for 12 h, followed by washing with deionized water. These films were treated with 0.005 M AgNO_3 solution, washed and reduced by hydrazine solution ($50\ \mu\text{L}$ in 30 mL of water) in a glove bag. The excess hydrazine was washed out, and the films were ion-exchanged with 1 M NaCl solution to remove unreacted silver ions from the zeolite framework.

2.8. Biological studies

To test the antibacterial activity of micropatterned silver-zeolite films, cultures of XL-1 blue *E. coli* were incubated with the disks and assessed for viability using traditional colony counts. LB broth solution was prepared using a concentration of 25 g/L. LB agar plates were prepared with 1.5% agar. Individual clones were inoculated in 3 mL of LB broth and shaken at 225 rpm overnight at 37°C . Prior to exposing bacteria to the zeolite membranes, bacterial cultures were adjusted to obtain an initial optical density (OD) of ~ 0.10 . Patterned-zeolite films with or without silver nanoparticles were placed into 24 well tissue culture plates, and 2 mL of bacterial suspension was added to each well, including wells with bacteria only. Experimental plates were incubated at 37°C and continuously shaken. Samples were removed, serially diluted and plated on LB agar at 0, 30, 60, 120, and 180 min. LB plates were incubated at 37°C overnight and colony forming units were counted to determine bacteria viability.

3. Results and discussion

Techniques for micropatterning or microfabrication of ceramics are of current interest. For patterning done by micromolding in

capillaries (MIMIC), low viscosity precursor solutions needed to be used, often resulting in shrinkage of the final structures which led to cracks. The molds for the process described in this paper were fabricated by replicating the photoresist pattern on a silicon wafer with PDMS or PMMA. For the first set of experiments, a simple PDMS micropattern was chosen, with parallel lines of $5 \times 5\ \mu\text{m}$ (width \times height) separated by $45\ \mu\text{m}$ gaps. These surface microfeatures were successfully introduced on the alumina supports, in agreement with previous studies [15].

Fig. 1 is a schematic representation of the entire process using the PDMS mold. Fig. 2(a) shows a micrograph of the sintered alumina, patterned using the PDMS molds. In order to obtain crack-free patterns, the key parameters were choice of solid alumina loading in the slurry, use of appropriate dispersant and controlled drying. The high loading of 80 wt.% of alumina in the slurry resulted in good pattern transfer with minimal shrinkage. The zeolite seed layer on the alumina support was formed using nanocrystalline zeolite Y ($\sim 200\ \text{nm}$). This seed layer was grown into a film by hydrothermal secondary growth at 90°C for 7 days. The zeolite/alumina needed to be calcined carefully ($0.2^\circ\text{C}/\text{min}$) to avoid cracking of the zeolite film. The zeolite film followed the pattern of the alumina support. The conformal nature of the coating can be better appreciated when comparing the cross-section of uncoated and zeolite-coated substrates (Fig. 2a inset and Fig. 2d). Cross sectional analysis of the samples via SEM confirmed that the zeolite film had a thickness of $2\text{--}3\ \mu\text{m}$ (Fig. 2d).

With finer features in the PDMS molds, it was difficult to maintain these features in the alumina without defects. In particular, manual demolding of the alumina from the PDMS in the green form often led to surface defects, presumably due to a high contact force between the PDMS and the nanostructured alumina, and the weak mechanical properties of the unsintered ceramic. An alternative strategy using PMMA molds was examined. Fig. 3 shows a step-by-step diagram of the process based on the use of PMMA molds, starting with the PDMS mold, and finally with the zeolite coating on the patterned surface of the alumina support. Gradual and slow removal of the PMMA mold via pyrolysis allowed the alumina to gain strength as it was being demolded, which resulted in better preservation of the surface micropatterns. Fig. 4 shows the results obtained with a more complex pattern using the PMMA

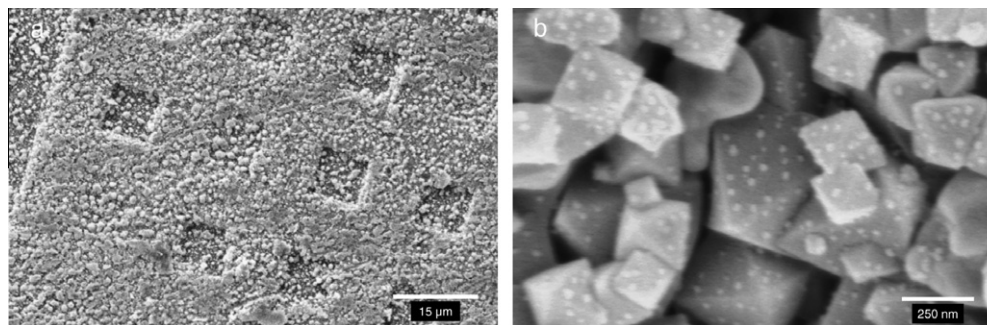


Fig. 5. SEM micrographs of (a) the zeolite film after growth of silver particles and (b) a magnified image of the surface. (Note that the SEM is from the right of the black square in Fig. 4 with grooves above the PDMS plane).

method. Focusing on the square pattern (Fig. 4a), dimensional changes were noted at each step, which were significant when going from the PMMA mold to sintered alumina. In the PDMS mold, the size of the square was $10.28 \pm 0.08 \mu\text{m}$ on each side with a height of $1.1 \pm 0.07 \mu\text{m}$ (Fig. 4b). Upon transferring the pattern to PMMA, the length and height/depth of the square remained unaltered at $10.26 \pm 0.16 \mu\text{m}$ and $0.98 \pm 0.04 \mu\text{m}$, respectively (Fig. 4c). For the alumina film, the length of the square shrank to $9.11 \pm 0.05 \mu\text{m}$ with a height of $1.03 \pm 0.05 \mu\text{m}$ (Fig. 4d). The shrinkage is a result of the sintering of the alumina. With the zeolite Y film, the length of the square increased to $10.43 \pm 0.30 \mu\text{m}$, with a height of $1.32 \pm 0.05 \mu\text{m}$ (Fig. 4e). The granular nature of the zeolite coating made accurate measurement of dimensions difficult; however, as expected the zeolite coverage did increase the size of the pattern. Fig. 4f also shows the powder X-ray diffraction of the zeolite Y film on the alumina support. The peak at $6^\circ 2\theta$ is due to the zeolite and the peak at $25^\circ 2\theta$ is due to the alumina.

Silver clusters were incorporated into the zeolite film by ion-exchange with Ag^+ , followed by reduction with hydrazine [23]. Fig. 5 shows the SEM of the Ag particles on the silver film at two different magnifications. The pattern on the zeolite film in Fig. 5a exhibits depressed squares, arising from the pattern to the right of the marked square in the PDMS mold in Fig. 4a. Ag nanoclusters are anchored on the surface of the zeolite with sizes $<50 \text{ nm}$ and also embedded within the matrix.

The biological studies were conducted using the patterned films containing Ag (Fig. 4). These films were examined for their antimicrobial property.

Silver is known as an excellent antimicrobial agent [24,25]. Prior to the experiments with bacteria, the zeolite films were re-exchanged with Na^+ to remove any unreacted Ag^+ ions. Antimicrobial activity of the patterned films was performed against *E. coli*. Fig. 6 shows the *E. coli* viability over time and compares bacteria alone with the patterned zeolite and patterned Ag-zeolite. The experiment was carried out over a period of three hours. With both bacteria alone and the patterned zeolite, bacterial populations increased approximately by a factor of ten, but with the Ag-zeolite film, bacteria were all dead in a period of 120 min. Antibacterial experiments were performed on three independent patterned silver zeolite membranes, with essentially identical results. The silver zeolite composite prevents the agglomeration of silver particles and should limit the release and dispersal of the nanoparticles, providing better environmental long-term stability. In other Ag immobilization studies, nanoclay Ag composites are reported to be efficient antimicrobials, and the mechanism of action was via membrane disruption from the generation of reactive oxygen species (ROS) [26]. Studies have also examined the antimicrobial activity of zeolite ion-exchanged with Ag^+ (not Ag colloids), and the antimicrobial activity was proposed to be due to the formation of ROS [27]. The mechanism of bactericidal activity of our Ag colloid-zeolite films has yet to be definitively established, and will be the subject of future experiments.

The rationale for patterning was to create more surface area increasing the number of contact points with the bacteria. Micro-patterned aluminosilicate coatings with antibacterial properties on structural nanophase ceramics have significant potential in the field of bone implants, a current area of research in our laboratories. A number of ceramic materials, including alumina, zirconia, zirconia-toughened alumina, and alumina-toughened zirconia, have been actively studied and/or implemented in this field due to their excellent mechanical and cytocompatibility properties, among others [28]. However, different strategies are still being explored to improve the osseointegrability (i.e. ability to allow direct anchorage/adaptation of bone tissue to its surface) of these materials. The use of zeolites and micro/nanopatterned material surfaces have been shown separately to be effective means of enhancing the osseointegration of bone materials [29]. Patterned-zeolite films and the controlled introduction of antimicrobial agents or other bioactive compounds within the zeolite film provides the possibility to elicit favorable biological responses (e.g. prevent infections, stimulate cell genesis or differentiation) that could help to increase the success rate of bone implants [30].

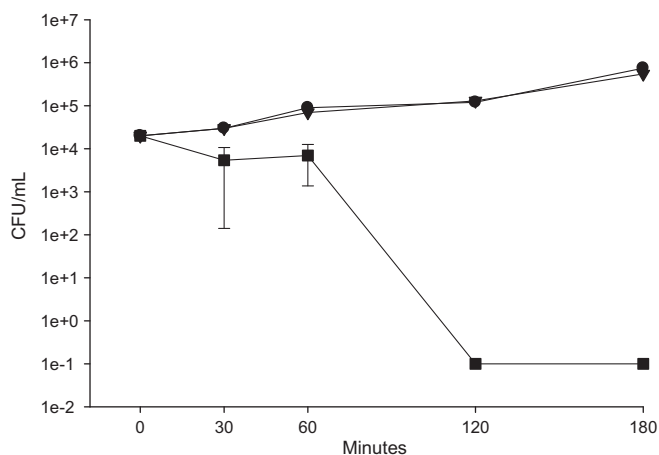


Fig. 6. *E. coli* was incubated alone (—●—), with patterned zeolite membranes (—▼—) or with patterned-zeolite films with Ag^0 nanoparticles that was Na^+ exchanged (—■—). Samples were examined over three hours to determine their antibacterial effects. Bars represent the standard deviations of three membranes; at 120 and 180 min all three membranes exhibited complete killing.

4. Conclusions

We have successfully demonstrated the fabrication of crack-free, complex alumina microstructures (5–100 μm) with soft lithog-

raphy techniques. Zeolite films (2–3 μ) were grown on the patterned alumina supports, and followed the alumina pattern. Silver nanoparticles were stabilized on patterned zeolite membrane and antibacterial properties of silver patterned zeolite membranes on *E. coli* were found to be potent and efficient, with complete eradication within 120 min, although the bactericidal mechanism of these materials is still being studied.

Acknowledgements

The *E. coli* was a kind gift from Dr. Joanne Trgovcich at The Ohio State University. We acknowledge funding from NIOSH Grant R01 OH009141 and AFOSR MURI Grant F49620-03-1-0421.

References

- [1] D.W. Breck, Zeolite molecular sieves: structure, chemistry and use, John Wiley & Sons, Inc., 1974.
- [2] S. Auerbach, K.A. Carrado, P.K. Dutta, Handbook of Zeolite Science and Technology, Marcel Dekker Inc., New York, 2003.
- [3] J.H. Koegler, H.W. Zantbergen, J.L.N. Nieuwenhuizen, M.S. Jansen, J.C. Jansen, H. Van Bekkum, Stud. Surf. Sci. Catal. 84 (1994) 307–314.
- [4] J.L.H. Chau, C. Tellez, K.L. Yeung, K.-C. Ho, J. Membr. Sci. 164 (2000) 257–275.
- [5] K. Kusakabe, S. Yoneshige, A. Murata, S. Morooka, J. Membr. Sci. 116 (1996) 39–46.
- [6] Y.S.S. Wan, J.L.H. Chau, A. Gavriilidis, K.L. Yeung, Micro. Meso. Mater. 42 (2001) 157–175.
- [7] J.N. Armor, J. Membr. Sci. 147 (1998) 217–233.
- [8] W.M. Moreau, Semiconductor Lithography: Principles and Materials, Plenum, New York, 1988.
- [9] Y. Xia, G.M. Whitesides, Annu. Rev. Mater. Sci. 28 (1998) 153–184.
- [10] W.S. Beh, Y. Xia, D. Qin, J. Mater. Res. 14 (1999) 3995–4003.
- [11] D. Zhang, B. Su, T.W. Button, Adv. Eng. Mater 5 (2003) 924–927.
- [12] B.D. Gates, Q. Xu, J.C. Love, D.B. Wolfe, G.M. Whitesides, Annu. Rev. Mater. Res. 34 (2004) 339–372.
- [13] Z. Zhu, X. Wei, K. Jiang, J. Micromech. Microeng. 17 (2007) 193–198.
- [14] Z. Zhang, F.F. Lange, Adv. Eng. Mater 4 (2002) 294–295.
- [15] U.P. Schönholzer, L.J. Gauckler, Adv. Mater 11 (1999) 630–632.
- [16] U.P. Schönholzer, R. Hummel, L.J. Gauckler, Adv. Mater 12 (2000) 1261–1263.
- [17] D. Zhang, B. Su, T.W. Button, J. Eur. Ceram. Soc. 24 (2004) 231–237.
- [18] Y.L.A. Leung, K.L. Yeung, Chem. Eng. Sci. 59 (2004) 4809–4817.
- [19] J.L.H. Chau, A.Y.L. Leung, K.L. Yeung, Lab Chip 3 (2003) 53–55.
- [20] Q. Li, M.L. Amweg, C.K. Yee, A. Navrotsky, A.N. Parikh, Micro. Meso. Mater 87 (2005) 45–51.
- [21] J.L.H. Chau, K.L. Yeung, Chem. Commun. (2002) 960–961.
- [22] L. Huang, Z. Wang, J. Sun, L. Miao, Q. Li, Y. Yan, D. Zhao, J. Am. Chem. Soc. 122 (2000) 3530–3531.
- [23] P.K. Dutta, D. Robins, Langmuir 7 (1991) 2004–2006.
- [24] M. Rai, A. Yadav, A. Gade, Biotechnol. Adv. 27 (2009) 76–83.
- [25] Y. Matsumura, K. Yoshikata, S.I. Kunisaki, T. Tsuchido, Appl. Environ. Microbiol. 69 (2003) 4278–4281.
- [26] H.L. Su, C.C. Chou, D.J. Hung, S.H. Lin, I.C. Pao, J.H. Lin, F.L. Huang, R.X. Dong, J.J. Lin, Biomaterials 30 (2009) 5979–5987.
- [27] Y. Inoue, M. Hoshino, H. Takahashi, T. Noguchi, T. Murata, Y. Kanzaki, H. Hamashima, M. Sasatsu, J. Inorg. Biochem. 92 (2002) 37–42.
- [28] G. Balasundaram, T.J. Webster, J. Mater Chem. 16 (2006) 3737–3745.
- [29] R.S. Bedi, L.P. Zanello, Y. Yan, Adv. Func. Mater 19 (2009) 3856–3861.
- [30] A. Dahm, H. Eriksson, J. Biotechnol. 111 (2004) 279–290.